Journal of Statistical Physics, Vol. 36, Nos. 3/4, 1984

Nucleation and Metastability in Three-Dimensional Ising Models[1]

Dieter W. Heermann,[2,3] Antonio Coniglio,[2,4] W. Klein,[2] and Dietrich Stauffer[2,5]

Received October 25, 1983; revised March 6, 1984

We present Monte Carlo experiments on nucleation theory in the nearest-neighbor three-dimensional Ising model and in Ising models with long-range interactions. For the nearest-neighbor model, our results are compatible with the classical nucleation theory (CNT) for low temperatures, while for the long-range model a breakdown of the CNT was observed near the mean-field spinodal. A new droplet model and a zeroth-order theory of droplet growth are also presented.

KEY WORDS: Classical nucleation theory; droplet definitions; lattice gas; Monte Carlo; spinodal.

1. INTRODUCTION

For systems which exhibit a first-order phase transition, e.g., water, the Ising model or a lattice gas one distinguishes three types of regions: The region outside the coexistence curve, which is absolutely stable, the spinodal region, which is absolutley unstable, and a region between these two, which is metastable. In mean field theories such as the van der Waals theory for fluid systems, or the Pierre Weiss theory of ferromagnetism, the metastable and unstable region are separated by a sharp boundary, the spinodal. However,

[1] Supported in part by grants from ARO, ONR, and NSF.

[2] Center for Polymer Studies and Department of Physics, Boston University, Boston, Massachusetts 02215.

[3] Now at Institut für Festkörperforschung, Theorie II, Kernforschungsanlage Jülich, Postfach 1913, D-5170 Jülich 1, West Germany.

[4] Permanently at Instituto di Fisica Teorica, Universita di Napoli, Mostra d'Oltremare, Pad. 19, 80125 Napoli, Italy.

[5] Permanently at Institut für Theoretische Physik, Universität zu Köln, Köln, West Germany.

0022-4715/84/0800-0447$03.50/0

thus far no evidence for the existence of such a sharp boundary has been found, and also classical nucleation theory[1,2] does not predict a well-defined spinodal. Instead, experimental data have been interpreted in terms of pseudospinodals.[3] Such pseudospinodals are obtained by extrapolations, but this does not constitute evidence for an actual spinodal.[4] It is now believed[4] that there is no sharp boundary between the unstable and metastable region. Rather, a "fuzzy" region separates them where there is a gradual transition from nucleation to spinodal decomposition.

Here we present Monte Carlo simulations of the metastable states of three-dimensional Ising models with short-range interactions, i.e., the usual nearest-neighbor model, and with long-range interactions. In all the models the order parameter is not conserved (Glauber dynamics). In particular, we address the question of the existence of a spinodal and investigate how far nucleation theory can describe the metastable states.

The outline of this paper is as follows. In Section 2 some aspects of the classical nucleation theory of Becker and Döring are briefly reviewed. The results of Monte Carlo calculations on the droplet distribution, nucleation rate, and droplet for the nearest-neighbor three-dimensional Ising model are presented in Section 3. Section 4 is devoted to Monte Carlo studies of the metastable states in Ising models with long-range interactions. A new droplet model which predicts a percolation transition at the mean field spinodal is presented in Section 5, and in Section 6 growth of noncompact droplets is studied.

2. CLASSICAL NUCLEATION THEORY

To set the stage for the Monte Carlo calculations we briefly review some aspects of the classical nucleation theory of Becker and Döring[1,2] (for detailed reviews see J. D. Gunton *et al.*[5] or Zettlemoyer[6]).

Let n_s be the average number of droplets of size s, R_s the rate of condensation of monomers for droplets of size s, and R_s' the evaporation rate. The rate J_s per unit volume at which droplets of size s grow to droplets of size $s+1$ is given by

$$J_s = R_s n_s - R_{s+1}' n_{s+1} \tag{2.1}$$

and we can write the continuity equation

$$\partial n_s(t)/\partial t = J_{s-1} - J_s, \qquad s \geqslant 2 \tag{2.2}$$

and thus obtain for the stationary state

$$J = J_1 = J_2 = \cdots \tag{2.3}$$

a nucleation rate independent of the droplet size s. Assuming (i) that the number of droplets of size s is related to the formation free energy F_s by

$$n_s \propto \exp(-F_s/k_B T) \tag{2.4}$$

and (ii) that

$$F_s/k_B T = \Gamma s^{2/3} - hs \tag{2.5}$$

one obtains the nucleation rate

$$J \propto n_s^* \propto \exp(-4\Gamma^3/27h^2) \tag{2.6}$$

h is the applied field [$h = 2$ (magnetic dipole moment) (magnetic field)$/k_B T$] and measures the distance to the coexistence curve ($h = 0$). For vapor-to-liquid nucleation one would use the chemical potential instead of the magnetic field.

The critical nucleus, s^*, is the droplet size where the free energy $F_s/k_B T$ has a maximum. The maximum of F_s constitutes an activation energy barrier. Droplets below the critical size will tend to shrink. Droplets larger than the critical size will predominately grow, decreasing the free energy and leading the system out of a metastable state to a stable equilibrium state.

Equation (2.4) is, however, only exact in the limit $J \to 0$ and $h \to 0$. For nonzero field and nucleation rate Eq. (2.4) is an approximation.

In (ii) the droplets are assumed to be compact and spherical in contrast to a ramified structure. The first term is the surface free energy with Γ related to the bulk surface tension σ associated with the interface between the up and the down spins by $\Gamma = (36\pi)^{1/3}\sigma/k_B T$. σ is taken to be a constant, equal to the tension of a flat interface and independent of the quenching parameter. As has been pointed out,[7] such a procedure is only valid in the limit $h \to 0$, i.e., close to the coexistence curve. The second term is the contribution from the bulk free energy, i.e., the energy required to flip s spins.

3. NUCLEATION IN THE NEAREST-NEIGHBOR THREE-DIMENSIONAL ISING MODEL

In two dimensions, computer simulations[4,8,9] close to the critical point confirmed the general concept of nucleation theory as described in the previous section. Simulations of three-dimensional systems[10,11] concentrated on the growth of droplets after nucleation or did not measure the nucleation rate quantitatively. Here we want to report on Monte Carlo simulations of the droplet size distribution, the nucleation rate, and the

growth of droplets in the three-dimensional nearest-neighbor Ising model (see Appendix A for the method).

Nucleation theory for Ising models requires a definition or model of a droplet. These droplets do not necessarily represent "physical droplets".[8] We assume in the following discussions that the droplets (the term "cluster" will be used synonymously with droplet) are formed by the "up" spins in a sea of "down" spins. In our simulations we have used two droplet models, the usual Ising droplets and modified droplets[12]:

Definition 3.1: Ising Droplets. Two "up" spins belong to the same droplet if they are nearest neighbors.

Definition 3.2: Modified Droplets. Two "up" spins belong to the same droplet if they are nearest neighbors and if there is a bond present between these two spins.

Bonds between nearest-neighbor "up" spins are present with a probability

$$P_B = 1 - \exp(-2J/k_B T) \tag{3.1}$$

where J is the exchange energy, k_B the Boltzmann constant, and T the temperature.

While bonds between nearest-neighbor "up" spins are always present in the Ising droplet picture, they are diluted with a probability P_B in the modified droplet picture. This has the effect of either reducing the size or breaking up the Ising droplets into smaller ones.

From the work of Müller-Krumbhaar[13] it is known that the Ising droplets undergo a percolation transition on the coexistence line at a temperature $T/T_c = 0.96$. The modified droplet model, on the other hand, predicts percolation to occur at the critical temperature T_c. At T_c we have

$$P_B = 0.358 \tag{3.2}$$

which was shown to be in good agreement with computer simulations.[14] In addition they satisfy the conditions

1. that their linear dimension, i.e., the connectedness length, diverges as the Ising correlation length, and
2. the mean cluster size diverges with the susceptibility.[15,16]

These conditions are necessary for a proper droplet model. In Section 5 we present an extension of the modified droplet definition which predicts the

percolation transition to coincide with the mean field spinodal and reduces to the definition given above at the critical temperature.

Three temperatures were selected for our studies, $T/T_c = 0.59$ ($J/k_B T = 3/8$), 0.86, and 0.96. Part of the results for $T/T_c = 0.59$, which was also used by Kalos *et al.*[11] have been reported in a previous paper[17] and will be given here in more detail. At $T/T_c = 0.96$ the Ising droplet picture is expected to break down due to the percolation transition.

3.1. Droplet Distribution

In the limit of large droplets with size s much smaller than the critical size s^* we expect from classical nucleation theory a distribution [see Eq. (2.4)]

$$n_s \propto \exp(hs - \Gamma s^{2/3}) \tag{3.1.1}$$

Taking the logarithm, we get

$$\ln n_s - hs = -\Gamma s^{2/3} + a \tag{3.1.2}$$

where a comprises the proportionality factor in (3.1.1). Classically a is taken to be the number density of monomers. In a semilogarithmic plot we therefore should get a straight line for our Monte Carlo data of the droplet size distribution. Figures 1a–1c show the results for various quench depths for the temperature $T/T_c = 0.59$ using the Ising droplet definition, and Fig. 1d using the modified droplet definition. We see that indeed a straight line can be fitted to our data for large droplets in both cases. Only the small droplets do not obey the relation predicted by Eq. (3.1.1), which is not surprising since the assumption of a compact droplet is not expected to hold for small droplets. For such small "droplets," consisting of 10 or less monomers, Kalos *et al.*[11] and Marro and Toral[11a] found empirical formulas for these clusters. The deviation for the field $h = 0.6$ can be explained quantitatively by the difference between equilibrium and stationary state.

For the temperature $T/T_c = 0.86$ (cf. Figs. 2a and 2b) our results are similar to those described above.

On the coexistence curve the Ising droplets undergo a percolation transition at $T/T_c = 0.96$. There the droplet distribution is expected to be

$$n_s \propto s^{-\tau} \tag{3.1.3}$$

From our Monte Carlo data we find (see Fig. 3) the exponent τ bo be

$$\tau = 2.16 \tag{3.1.4}$$

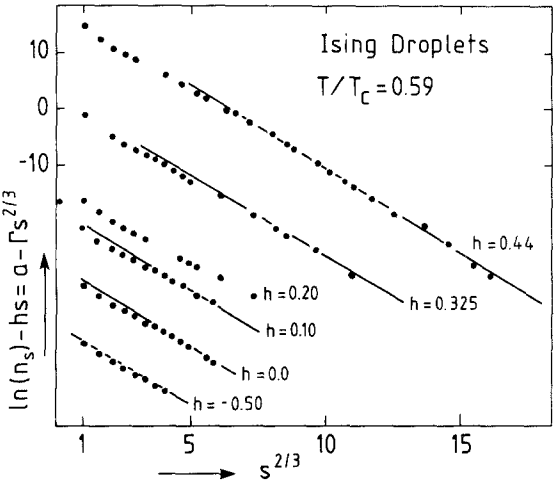

(a)

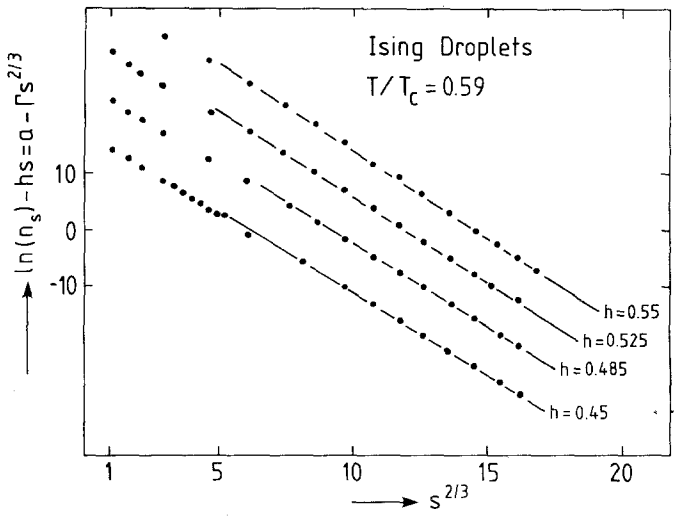

(b)

Fig. 1. Variation of the surface part of the droplet formation energy F_s $[hs - \ln(n_s)]$ with the droplet surface $s^{2/3}$, (a–c) using the Ising droplets and (d) using the modified droplet definition. The temperature was $T/T_c = 0.59$. The large droplets obey approximately the prediction of the classical nucleation theory. The resulting surface tension seems to be independent of the applied field since all lines are nearly parallel.

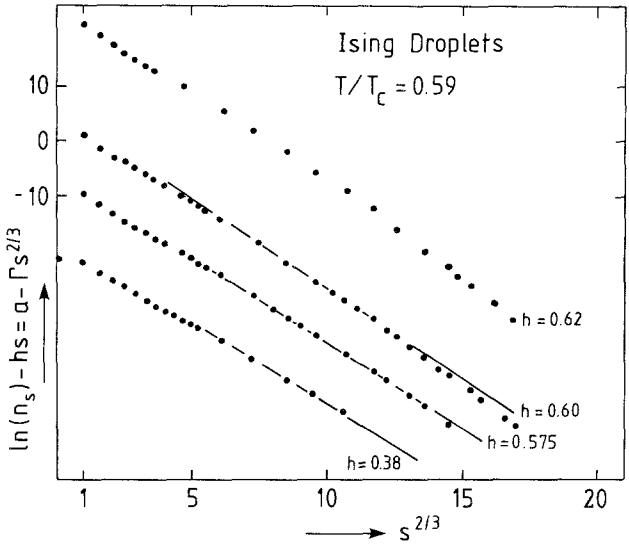

(c)

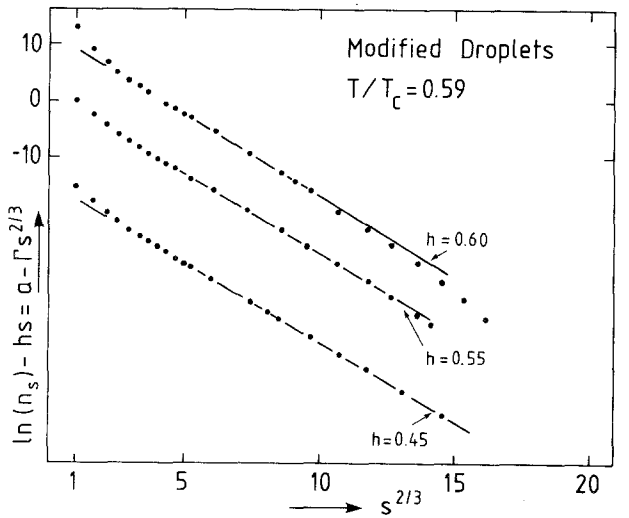

(d)

Fig. 1 (*continued*)

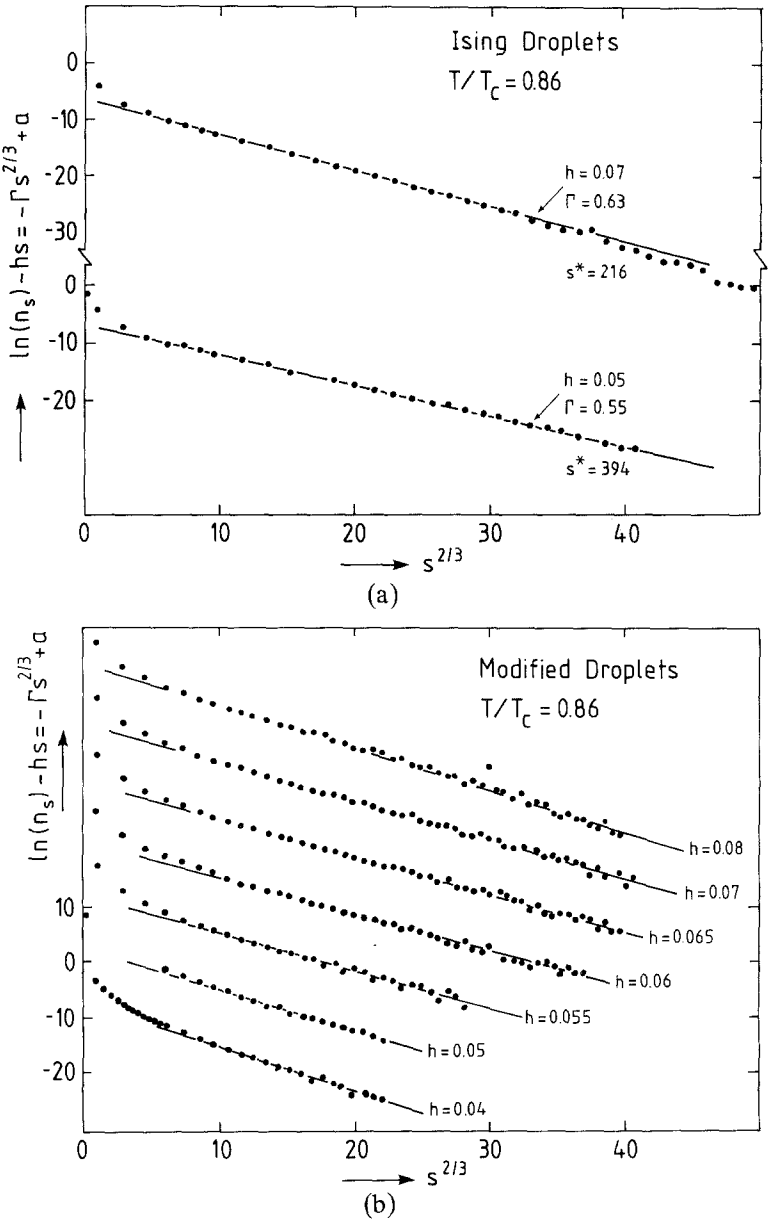

Fig. 2. Variation of the surface part of the droplet formation energy F_s $[hs - \ln(n_s)]$ with the droplet surface $s^{2/3}$, (a) using the Ising droplet definition at $T/T_c = 0.86$ and (b) using the modified droplet definition. The large droplets obey approximately the prediction of the classical nucleation theory. The resulting surface tension seems to be independent of the applied field since all lines are nearly parallel.

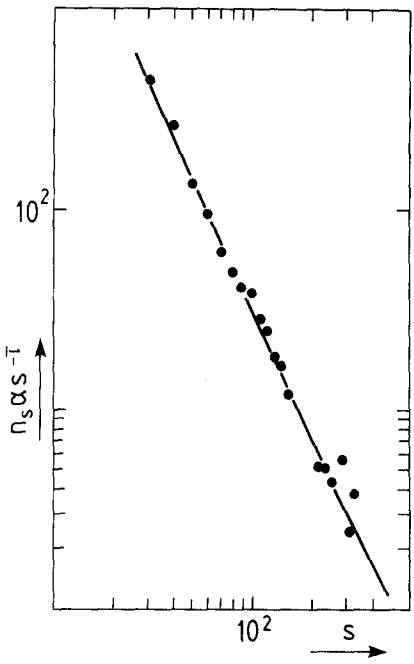

Fig. 3. Log–log plot of the number of droplets of size s as a function of s using Ising droplets for the temperature $T/T_c = 0.96$ with zero applied field. The exponent $\tau = 2.16$ is consistent with values reported in the literature for the percolation threshold.

which is consistent with the values given in the literature ($\tau = 2.19$, Stauffer,[18] Reeve[19]). For comparison we have made in Fig. 4 the same plot as for the temperatures $T/T_c = 0.59$ and 0.86.

The parallel lines in Figs. 1, 2, and 4 suggest that the surface tension is independent of the applied field h for both Ising and modified droplets as assumed in the classical nucleation theory (see also Fig. 5, where the critical droplet size s^* obtained from the simulations is plotted versus $1/h^3$). However, it should be noted that the applied fields are still close to the coexistence curve compared to the mean field spinodal field ($h = 1.43$). Table 1 comprises the surface tensions obtained by our Monte Carlo calculations and from different sources.

Γ_{sphere} and Γ_{cube} are obtained from F_s, the formation free energy, by assuming spherical or cubical shapes for the droplets. At $T/T_c = 0.59$ the surface tension of both Ising and modified droplets are compatible with the surface tension for a sphere obtained by series expansions and Monte Carlo simulations, and at the higher temperature the surface tensions for the Ising droplets agree with those of Γ_{sphere}. But due to the limited droplet size in our simulations, our data at $T/T_c = 0.96$ are not accurate enough to determine reliably the surface tension of Ising and modified droplets. The Ising droplets are consistent with both $n_s \propto s^{-\tau}$ (Fig. 3) and $\ln n_s \propto s^{-1/3}$ (Fig. 4a). In the

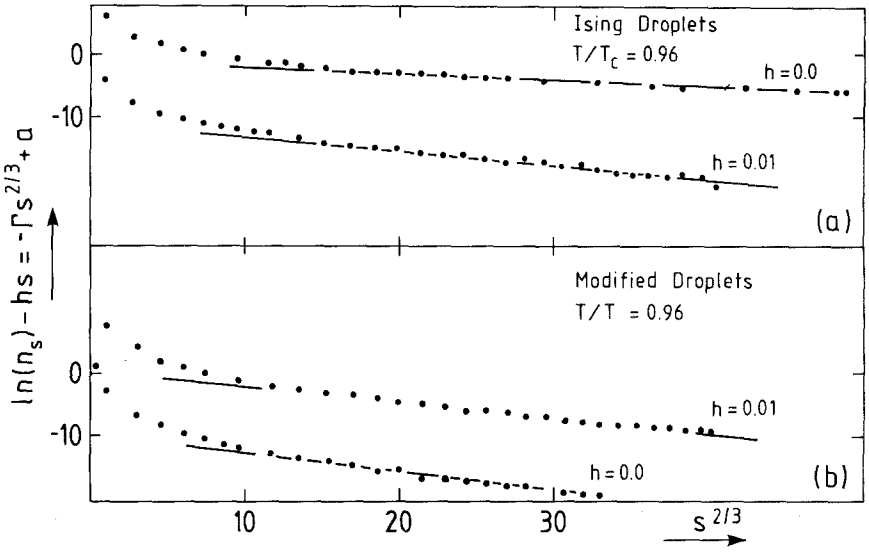

Fig. 4. Variation of the surface part of the droplet formation energy F_s with the droplet surface using (a) the Ising droplet definition and (b) the modified definition for the temperature $T/T_c = 0.96$.

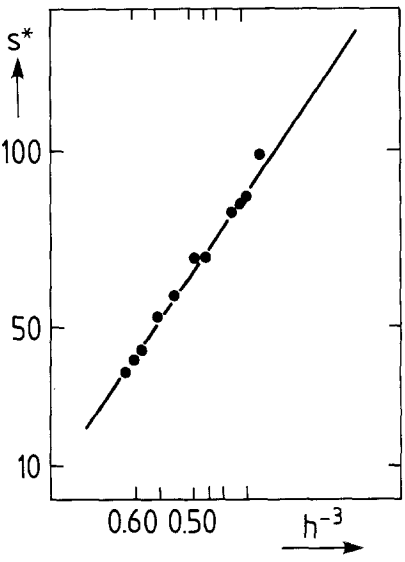

Fig. 5. Critical droplet size s^* obtained from the simulations versus $1/h^3$ for the temperature $T/T_c = 0.59$. Classical nucleation theory predicts $s^* = (2\Gamma/3h)^3$.

Table I

T/T_c	F_s	Γ_{sphere}	Γ_{cube}
0.59	0.574[a]	2.78	3.44
0.86	0.112[b]	0.54	0.67
0.96	0.016[b]	0.079	0.096
	0.02[c]	0.099	0.120

Monte Carlo data

	Ising		Modified	
T/T_c	Γ^d	Γ^e	Γ^d	Γ^e
0.59	3.0 ± 0.1	2.91 ± 0.1	2.85 ± 0.1	2.5 ± 0.1
0.86	0.59	—	0.72 ± 0.09	0.997 ± 0.08
0.96	0.085	—	0.275 ± 0.08	—

[a] From series expansion.[22]
[b] K. Binder, *Phys. Rev. A* **25**:1699 (1982).
[c] From E. Burgner and D. Stauffer, *Z. Phys.*, to be published.
[d] From $\ln(n_s) - hs = a - \Gamma s^{2/3}$.
[e] From $\ln(n_s) = a - (4/27)\Gamma^3 h^{-2}$.

latter interpretation the droplet surface tension agrees numerically with the bulk surface tension.[20,21]

3.2. Nucleation Rate

We saw in Section 1 that the experimentally important nucleation rate J, i.e., how many droplets overcome the nucleation barrier at the critical size s^*, is predicted by the classical nucleation theory to be

$$J \propto n_s^* \propto \exp(-4\Gamma^3/27h^2) \tag{3.2.1}$$

It should be noted that the nucleation rate was derived under the assumption of a steady state. In our simulations we could see this steady state and also the time lag until the steady state is achieved.

The comparison of the observed nucleation rates in the Ising model with the rate predicted by the classical nucleation theory is facilitated by the precise knowledge of the location of the coexistence curve. No error in the supersaturation, which would lead to fallacious predictions, is introduced, e.g., by an inaccurately known chemical potential on the coexistence curve.

The nucleation rate J determined by directly counting the number of

droplets overcoming the nucleation barrier, and determined from n_s^* for the temperature $T/T_c = 0.59$, is shown in Fig. 6. The straight line is the prediction from Eq. (3.2.1) where the classical prefactor was used and the surface tension was taken to be $=3.1$ (cf. Table 1). For small nucleation rates (small applied field) the data, however, indicate some curvature and are probably not just statistical fluctuations or finite size effects. Kehr and Binder[24] interpreted these deviations as being due to the transition from spherical to cubical droplet shape when the droplet size increases due to a decreasing field.

Deviation from the expected behavior of the nucleation rate was also found for the temperature $T/T_c = 0.86$ (cf. Fig. 7). The nucleation rate shows a curvature and not the expected linear behavior.

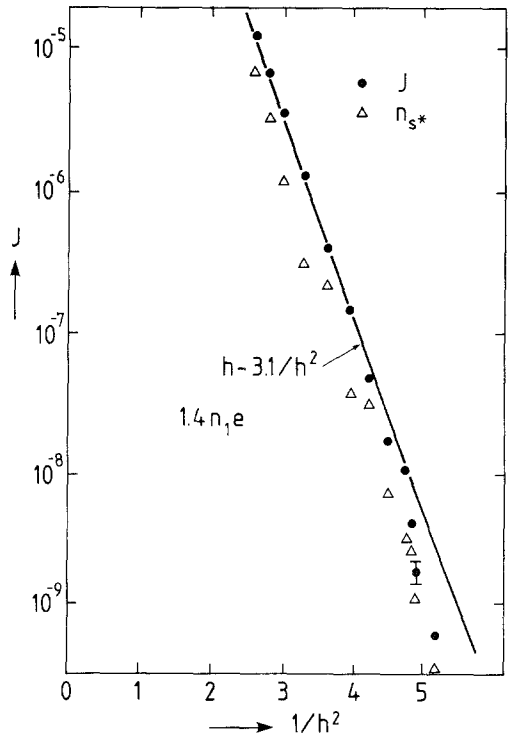

Fig. 6. Nucleation rate plotted logarithmically versus $1/h^2$ for the temperature $T/T_c = 0.59$. The solid line is the prediction from the classical nucleation theory with the surface tension $\sigma/k_B T$ taken from series expansions (Ref. 22). The crosses give the number n_s^* of critical nuclei, as found by our simulations. The dots give the observed nucleation rate.

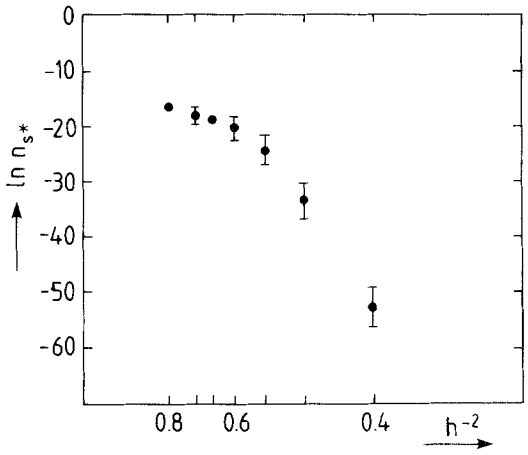

Fig. 7. Nucleation rate as determined by the number of droplets of critical size s^* versus $1/h^2$ for the temperature $T/T_c = 0.86$.

3.3. Growth of Droplets

Finally, let us look at the growth of droplets. According to classical nucleation theory, the growth of droplets after nucleation is governed by the difference of two terms: the incorporation rate and the evaporation rate of monomers, i.e., spins. This approximation should be valid, however, only in the early stages of the growth when the average supersaturation does not change appreciably and for low supersaturations. In the late stages of growth coagulation becomes important due to excluded volume effects.

One takes the incorporation rate and the evaporation rate proportional to the surface area of the droplet, i.e., to $s^{2/3}$. Then the droplet radius, for large s, increases linearly with time. Assuming further that dF_s/ds varies as $s^{-1/3}$ for large s, we obtain

$$(d/dt)s^{1/3} = \text{const}_1 - \text{const}_2\, s^{-1/3} \tag{3.3.1}$$

Figure 8 shows a typical growth process at $T/T_c = 0.59$ and a field $h = 0.45$. After overcoming the nucleation barrier, the droplet grows monotonically and eventually the droplet radius increases linearly with time. In Fig. 8b this growth process is shown for a temperature $T/T_c = 0.86$ and $h = 0.06$. In both cases the modified droplet definition was used. Runs with the Ising definition gave almost the same result.

The above result [Eq. (3.3.1)] was derived under the assumption of a

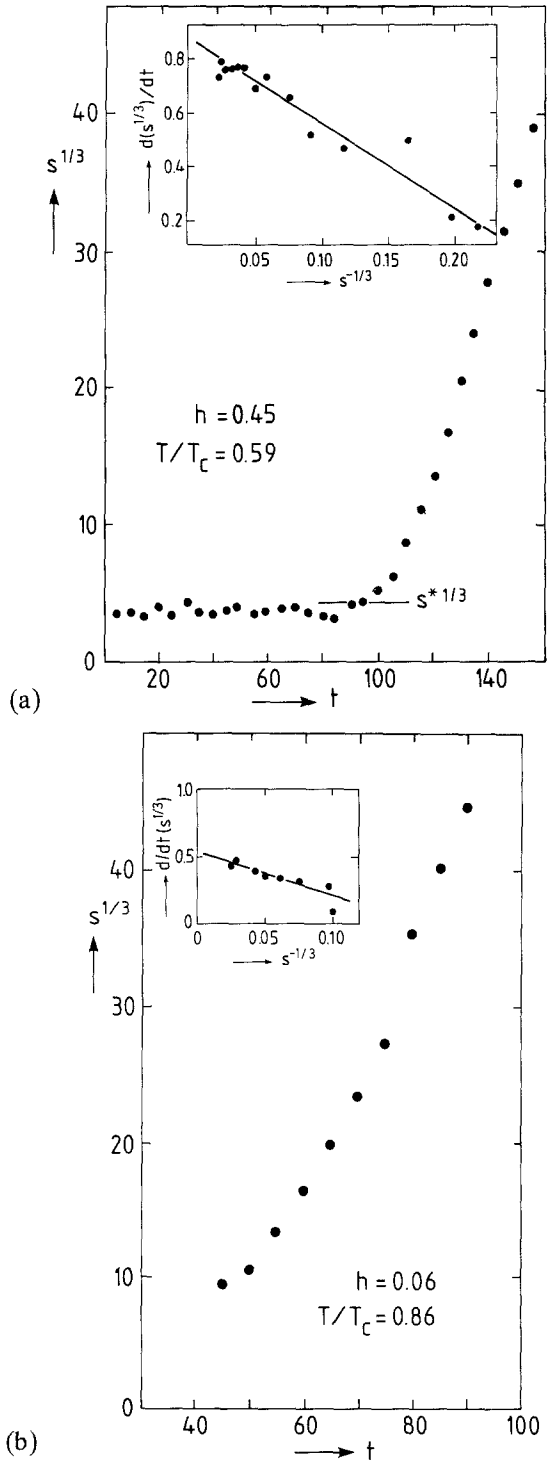

Fig. 8. Typical growth process of droplets after nucleation for (a) $T/T_c = 0.59$, $h = 0.45$, and (b) $T/T_c = 0.86$, $h = 0.06$.

compact droplet. In the case of noncompact droplets we expect a different growth law. A zeroth-order theory for this case will be presented in Section 6.

4. NUCLEATION IN LONG-RANGE THREE-DIMENSIONAL ISING MODELS

Despite the deviation for small nucleation rates the classical nucleation theory seems to work quite satisfactorily in Ising models with short-range interaction at low temperatures and for quenches not too deep into the metastable region. Deep quenches are not possible since no metastable equilibrium can be established. Here we investigate nucleation in Ising models with long-range interactions at low temperatures.

In our Monte Carlo simulations (see Appendix A for the method), we used a model proposed by Domb and Dalton,[25] the equivalent-neighbor model. This model bridges short-range interactions, i.e., the usual nearest-neighbor model and infinite-range interactions. It is assumed that each spin i in a simple cubic lattice interacts with q neighbors with equal interaction energy J. The spin i does not interact with spins outside the range R. The interaction strength in the Monte Carlo calculations of the metastable states of this model was $K = J/k_B T = (9/4)(1/q)$. For $q = 6$, i.e., the nearest-neighbor Ising model K reduces to the value used in the calculations in Section 3. The system size was 32^3 with periodic boundary conditions. Within the limit of accuracy we could not detect finite size effects by using systems of size 24^3 and 48^3.

A consequence of mean field theory is the existence of a spinodal which separates the metastable from the spinodal region. This spinodal is defined by the locus of the points where

$$\chi = (1 - m^2)/[1 - T/T_c(1 - m^2)] \tag{4.1}$$

diverges. The susceptibility calculated from the classical nucleation theory

$$\chi \propto \sum_{s=1}^{s^*} s^2 \exp(hs - \Gamma s^{2/3}) \tag{4.2}$$

however, does not diverge. The critical droplet size

$$s^* = (2\Gamma/3h)^3 \tag{4.3}$$

remains finite! The results of the Monte Carlo simulations for the susceptibility (calculated by the fluctuations in the order parameter $\chi \propto \langle m^2 \rangle - \langle m \rangle^2$) for the nearest-neighbor model are shown in Fig. 9. The

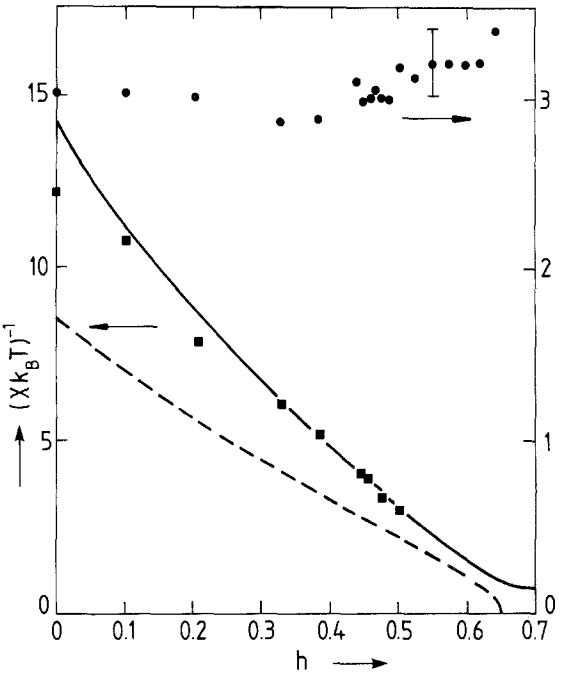

Fig. 9. Inverse susceptibility as a function of the applied field for $T/T_c = 0.59$ in the case of nearest-neighbor interactions. The solid curve is the prediction from the classical nucleation theory and the dashed line is the mean field prediction. The dots give the observed surface tension.

solid curve is the prediction of the classical nucleation theory, i.e., Eq. (4.2), where we have used $\Gamma = 3$ (see Table 1) and fitted the curve with the proportionality factor as the only free parameter on our susceptibility data. As expected from the results of Section 3 the agreement between classical nucleation theory and our data is quite good, but the data do not reach deep enough into the metastable region to indicate the existence of a spinodal or a bend over as suggested by the classical nucleation theory. The nearest-neighbor Ising model becomes unstable for deep quenches. No metastable equilibrium could be established due to the strong relaxation of the magnetization. Such a strong relaxation was also found for the two-dimensional nearest-neighbor Ising model[4] for deep quenches.

Let us now turn to long-range interactions[26] (see Fig. 10). The solid line represents the mean-field prediction for the inverse susceptibility from Eq. (4.1). The broken curve is the prediction of the classical nucleation theory for the temperature $T/T_c = 4/9$. The two free parameters, Γ and the proportionality factor were fitted near the coexistence curve. Fits were also

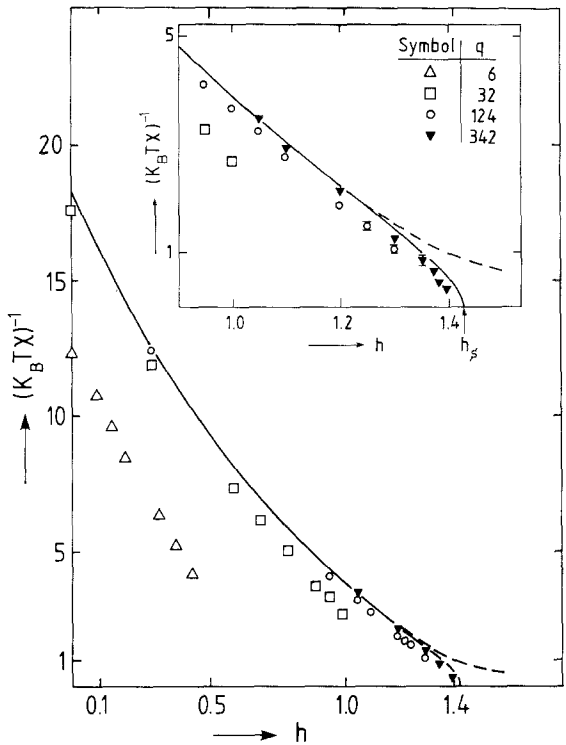

Fig. 10. Inverse susceptibility as a function of the applied field. The full curve is the mean-field prediction for $T/T_c = 4/9$. The spinodal is predicted at $h_s = 1.43$. The broken curve is a fit of the classical nucleation theory to the mean field prediction.

made deeper into the metastable region, which gave almost identical results. Surprisingly, the classical droplet model fits over a wide range. But near the mean-field spinodal, the classical nucleation theory breaks down as can be seen by the Monte Carlo results for $q = 342$. The data follows the mean-field prediction and do not bend over. The figure makes clear that the pseudospinodals converge very rapidly to the mean-field spinodal.

5. A NEW DROPLET MODEL

In Section 3 we used two droplet models, the Ising droplets and the modified droplets (see Definitions 3.1 and 3.2). Here we want to extend the definition of the modified droplets in such a way that the droplets diverge at the mean-field spinodal. The droplets used in nucleation theory of Becker and Döring do not have this property. Their radii stay finite at the spinodal.

But the droplets in the Cahn–Hilliard[7] theory of nucleation diverge at the mean-field spinodal.

It is clear that for long-range interaction the Ising droplets made of "up" spins pairwise within the range of interaction will exhibit a percolation transition on the coexistence curve at a temperature T_p well below the critical temperature. As the range of interaction goes to infinity $T_p \to 0$. How does one define a suitable droplet for very large-range interaction? We propose a modified droplet model in the following way: Two "up" spins belong to the same droplet if they are within the interaction range of each other and if there is a bond present between them. Bonds between interacting spins are active with a probability

$$P_B = 1 - \exp[-4J/k_B T(1-\rho)] \tag{5.1}$$

$\rho = (1+m)/2$ being the density.

We have calculated in the limit of infinite range interaction the mean droplet size $s = \sum s^2 n_s$ and found that

$$\bar{s} = 4(1-\rho) = [1 - 4(J/k_B T)\, q\rho(1-\rho)]^{-1} \tag{5.2}$$

where χ is the susceptibility of the Ising model in the mean field approximation and q is the number of neighbors with which a given spin interacts. In this limit $q \to \infty$ and $J \to 0$ such that Jq remains finite. From Eq. (5.2) follows that the mean droplet size diverges along the mean field spinodal, i.e., where χ diverges.

We have also calculated the droplet distribution n_s

$$n_s = \frac{1}{(2\pi)^{1/2}} \frac{1}{\lambda} s^{-5/2} \exp[-s(\lambda\rho - 1 + \ln\rho)] \tag{5.3}$$

where $\lambda = Jq$. Note that there is only one term proportional to s which vanishes at the spinodal. In computer simulations[27] we have evaluated the droplet size distribution and the mean droplet size for $q = 124$ and found good agreement with Eqs. (5.2) and (5.3) (cf. Fig. 11).

We briefly sketch the derivation of Eqs. (5.2) and (5.3). It is known that mean field results for the Ising model can be obtained by solving the model on the Bethe lattice with coordination number q and then taking the limit $q \to \infty$.[28] Using the general result developed for the site correlated random bond percolation on the Bethe lattice[29] with coordination number q, we have calculated in the limit $q \to \infty$, for a bond probability given by (5.1) the density of "up" spins in the infinite droplet

$$P = 1 - \exp[4P(J/k_B T(\, q\rho(1-\rho) - h] \tag{5.4}$$

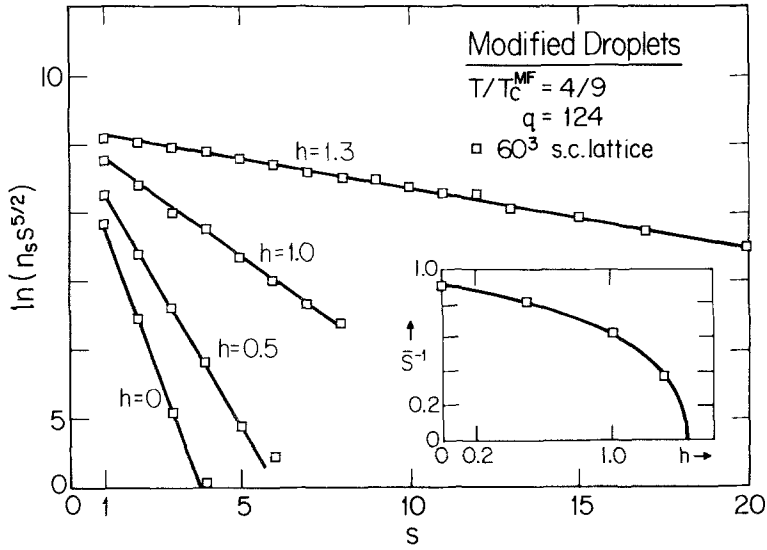

Fig. 11. Droplet size distribution n_s as a function of s for various magnetic fields. The solid lines are the predictions of Eq. (5.3). The inset gives the prediction for the mean droplet size as a function of the magnetic field (solid curve) and the data obtained by Monte Carlo simulations.

where h is a ghost field. The derivative with respect to h of P for $h=0$ is related to the mean droplet size $\bar{s}=(1-P)^{-1}(\partial P/\partial h)_{h=0}$, which leads to Eq. (5.2). Similarly we also obtain Eq. (5.3). It has also been shown[30] that a field theory representation of the spinodal can be mapped onto the field theory of the correlated site bond percolation model[31] and the results are consistent with those presented here.

6. RAMIFIED DROPLET GROWTH

In the growth of compact droplets the incorporation of monomers takes place only on the surface of the droplet. Each additional monomer contributes to the growth of the droplet radius. For more ramified droplets with an effective dimension d_+ not equal to d (the spatial dimension) additional monomers can contribute to either the growth of the radius or the effective dimension of the droplet. Moreover, the two processes can compete with each other for the available monomers in the environment.

In order to examine the effect of this competition, we investigate a very simple set of phenomenological equations which we believe retains the essential physics of this competition. We will assume, as above, that the difference between the capture and reevaporation rate is proportional to an

effective surface. Generally for ramified clusters we would take the surface proportional to the volume.[18,31] However, this would not account for the possible screening of the surface sites by neighboring sites.[32] This screening could result in an effective surface significantly smaller than the surface of the cluster. To account for this effect we will divide the ramified cluster with S spins into two parts. We imagine two concentric spheres centered at the center of mass of our cluster (see Fig. 12), which divides it into two zones.

In the outer sphere we will denote the number of spins by S_E and we assume that the spins in this zone are screened but not as much as in the interior. This reflects the fact that these spins far away from the center of mass of the cluster can be reached by monomers in the environment without significant "diffusion through the cluster." Since the actual cluster surface is proportional to the cluster volume, this leads to the equation

$$dS_E/dt = \beta S_E^y \tag{6.1}$$

where β includes all proportionality factors and $y < 1$.

In the interior zone the spins are more strongly screened and this leads to an equation of the form

$$dS_I/dt = \alpha S_I^x \tag{6.2}$$

where x is a parameter larger than y and S_I is the number of spins in the inner zone. The quantities S_I^x and S_E^y are measures of the effective surface available for incorporation of monomers. The value $x = 1$ corresponds to no screening. Clearly $S = S_I + S_E$. We also denote by S_I^* and S_E^* the values of S_I and S_E at time zero, i.e., when the nucleating droplet appears.

The radius of gyration R of the cluster is defined by

$$R^2 = (1/S) \sum_i r_i^2 \tag{6.3}$$

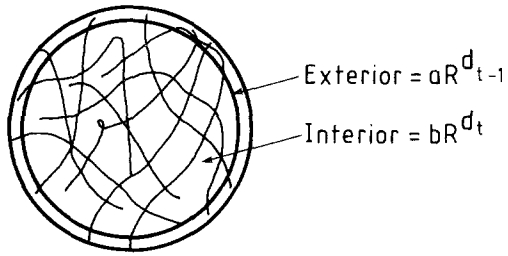

Fig. 12. Ramified droplet divided into two zones.

where r_i designates the distance of the ith spin from the center of mass of the droplet. We can then define an effective dimension d_+ by $R^{d_+} = S$ and define d_+^* to be its value at $t = 0$. The precise relationship between d_+ and the fractal dimension[33] is not clear, but the notion that d_+ specifies the "compactness" of the cluster is sufficient for our present purpose. We now take $S_E = aR^{d_+-1}$. The following points should be noted:

(1) The definition of d_+ will only make sense in the limit of large S. We will be restricted therefore to regions where $S^* \gg 1$.

(2) The region S_E is not well defined. Clearly there should be a smooth transition of degree of screening from the surface to the interior instead of a sharp boundary. In this work we take the unscreened region S_E equal to R^{d_+-1} for simplicity. Since we are presently attempting to qualitatively describe ramified droplet growth, this definition should be sufficiently precise for our purposes.

(3) The constants α, β, and x will generally be functions of time; however, for simplicity we will take them to be constants with respect to time. These variables will, however, be functions of S^*, S_I^*, and d_+^*. This can only be a reasonable approximation for short times, so we will restrict ourselves to a linear theory. With the above considerations it is easy to obtain

$$\ln R = \ln R^* + \alpha t(1-y)(R^*)^{d_+^*(1-y)} - \beta t/(1-x)(R^*)^{(d_+^*-1)(1-x)} \tag{6.4}$$

$$d_+ = d_+^* + t(\ln R[\alpha(1-d_+^*)/(1-y) + d_+^*\beta/(1-x)] \tag{6.5}$$

From Eqs. (7.4) and (7.5) we can distinguish three forms of growth depending on the values of x, α, β, S_s^*, S_I^*, and d_+^*:

a. d_+ grows and R shrinks;

b. R grows and d_+ shrinks;

c. both R and d_+ grow.

This is quite different from the growth of compact droplets where growth is defined by the increase in the droplet radius.

Finally we can ask, within the limits of the linear theory, for the time t_c at which $d_+ = d$. At t_c Eqs. (7.1) and (7.2) are valid and the growth takes place by the mechanism described earlier for compact droplet growth. From Eq. (7.5) we obtain

$$t_c = [\ln R^*(d-d_+^*) - C]\{[\alpha(1-d_+^*)/(1-y) + d_+\beta/(1-x)] + [\alpha/(1-y)(R^*)^{d_+^*(1-y)} - \beta(1-x)(R^*)^{(d_+^*-1)(1-x)}]\}^{-1} \tag{6.6}$$

If $d - d_{\pm}^{*}$ is small, then $t_c \ll 1$ and the droplet compactifies quickly. During this time R/R^* is roughly constant. This would imply that in medium-range interaction systems, in that region of the metastable state where $d_{\pm}^{*} = d$, the droplet compactifies on a time scale small compared to the time necessary for appreciable droplet growth. This is an important consideration in any experimental search for ramified droplets.

Although this model is crude, there is substantial evidence that the physical picture presented here is correct. Recent field theoretical studies of the early growth[34] produced results which are consistent with the conclusions reached here. Moreover, computer simulations[35,36] confirm the fact that the nucleating droplets are ramified and that the initial phase of growth is one of compactification.

7. SUMMARY

We have shown that the classical nucleation theory works quite well for the nearest-neighbor Ising model for low temperatures over a wide range of nucleation rates, although deviations for small rates imply some curvature. At higher temperatures the deviation from the expected behavior is stronger. The assumption of a surface tension independent of the applied field and the radius seems reasonable for the temperatures studied.

For Ising models with long-range interactions the classical nucleation theory was shown to break down in the vicinity of the mean-field spinodal.

ACKNOWLEDGMENTS

The authors would like to thank J. Marro, J. L. Lebowitz, F. Stillinger, and K. Binder for stimulating discussions.

APPENDIX A: NUMERICAL METHODS

The Monte Carlo simulations of Section 3 were done for a simple cubic lattice Ising model with nearest-neighbor interactions. In order to check for finite size effects, systems of size 168^3 and 120^3 were used. Within the experimental error no such effects could be determined. Using Glauber kinetics, a spin was flipped with probability $\exp(-\beta \Delta E)$, where ΔE is the energy connected with the flip and $1/\beta = k_B T$ is the thermal energy. For negative ΔE the spin was always flipped. Multispin coding with four bits per spin was used in the calculations and was then compressed to one bit per spin for storage.

We started with a configuration where all spins are down and then waited up to 20 Monte Carlo steps per spin for metastable equilibrium to be

established. Metastable equilibrium was created by an upward-oriented field h defined dimensionless through $h = 2$ (magnetic dipole moment) (magnetic field)$/k_B T$. Configurations were then periodically frozen and analyzed according to the droplet model. To avoid errors from droplet–droplet interactions the simulations stopped if more than 5% of the "up" spins belonged to droplets.

The simulations of Section 4 were carried out with a new algorithm. Here we briefly outline the basic idea of this algorithm. Instead of storing the spin orientation, one stores the sum $\sum_{(i,j)} s_i s_j$. If during the Monte Carlo process the spin at the site i is flipped, then this sum is updated for the site i and for the q neighboring spins.

APPENDIX B: TABLES OF THE MAGNETIZATION AND SUSCEPTIBILITY

$q = 32$			$q = 124$		
h	$-m$	$\chi k_B T$	h	$-m$	$\chi k_B T$
0	0.975	0.0569	0	0.975	0.0535
0.3	0.965	0.0838	0.3	0.965	0.0804
0.6	0.948	0.1357	0.95	0.920	0.2430
0.7	0.941	0.1626	1.0	0.913	0.2719
0.8	0.932	0.1982	1.05	0.906	0.3047
0.9	0.920	0.2653	1.1	0.898	0.3593
0.95	0.913	0.3027	1.2	0.876	0.5304
1.0	0.905	0.4315	1.225	0.869	0.5889
			1.25	0.862	0.6670

The interaction was $K = J/k_B T = (9/4)(1/q)$.

$q = 342$		
h	$-m$	$\chi k_B T$
1.05	0.908	0.2867
1.1	0.900	0.3427
1.2	0.880	0.4616
1.3	0.851	0.7849
1.35	0.828	1.1815
1.37	0.814	1.4207
1.38	0.807	2.118
1.40	0.773	—
1.41	0.767	—

REFERENCES

1. R. Becker and W. Döring, *Ann. Phys. (Leipzig)* **24**:719 (1935).
2. W. Döring, *Z. Phys. Chem.* **36**:317 (1937).
3. B. Chu, F. J. Schoenes, and M. E. Fisher, *Phys. Rev.* **185**, 185 (1969).
4. K. Binder, *Ann. Phys. (N.Y.)* **98**:345 (1976).
5. J. D. Gunton, M. San Miguel, and P. S. Sahni, in *Phase Transitions and Critical Phenomena*, (C. Domb and J. L. Lebowitz, Eds.) (Academic press, London, 1983).
6. A. C. Zettlemoyer, ed. *Nucleation I* (Dekker, New York, 1969).
7. J. W. Cahn and J. Hilliard, *J. Chem. Phys.* **31**:688 (1959).
8. K. Binder and D. Stauffer, *Adv. Phys.* **25**:345 (1976).
9. K. Binder and E. Stoll, *Phys. Rev. Lett.* **31**:47 (1973).
10. J. L. Lebowitz, J. Marro, and M. H. Kalos, *Acta Metall.* **30**:297 (1982).
11. M. H. Kalos, J. L. Lebowitz, O. Penrose, and A. Sur, *J. Stat. Phys.* **18**:39 (1978); O. Penrose, J. L. Lebowitz, J. Marro, M. H. Kalos, and A. Sur, *ibid.* **19**:243 (1978); O. Penrose and A. Buhagior, *ibid.* **30**:219 (1983).

11a. J. Marro and R. Toral, *Physica*, to be published.

12. A. Coniglio and W. Klein, *J. Phys. A* **13**:2775 (1980).
13. H. Müller-Krumbhaar, *Phys. Lett.* **50A**:27 (1975).
14. D. W. Heermann and D. Stauffer, *Z. Phys. B* **44**:339 (1980).
15. Roussenq, A. Coniglio, and D. Stauffer, *J. Phys. Lett.* (1982).
16. J. Kertesz, D. Stauffer, and A. Coniglio, *Ann. Israel Phys. Soc.* **5**:121 (1983).
17. D. Stauffer, A. Coniglio, and D. W. Heermann, *Phys. Rev. Lett.* **49**:1299 (1984).
18. D. Stauffer, *Phys. Rep.* **54**:1 (1979).
19. Reeve, *J. Phys. A* **15**:L521 (1982).
20. K. Binder, *Phys. Rev. A* **25**:1699 (1982).
21. H. Furukawa and K. Binder, *Phys. Rev. A* **26**:556 (1982).
22. F. H. Stillinger, private communication.
23. J. D. Weeks, G. H. Gilmer, and H. J. Leamy, *Phys. Rev. Lett.* **31**:549 (1973).
24. K. W. Kehr and K. Binder, in *Monte Carlo Methods in Statistical Physics*, Vol. II, edited by K. Binder (Springer, Berlin, 1984).
25. C. Comb and N. W. Dalton, *Proc. Phys. Soc.* **89**:859 (1966).
26. D. W. Heermann, W. Klein, and D. Stauffer, *Phys. Rev. Lett.* **47**:1262 (1982).
27. D. W. Heermann and W. Klein, *Phys. Rev. B* **27**:1732 (1983).
28. C. Domb, *Adv. Phys.* **9**:149 (1960).
29. A. Coniglio, H. E. Stanley, and W. Klein, *Phys. Rev. B* **25**:6805 (1982).
30. W. Klein and C. Unger, *Phys. Rev. B* **28** (1983).
31. A. Coniglio and T. C. Lubensky, *J. Phys.* **A13**:1783 (1980).
32. P. A. Rikvold, *Phys. Rev. A* **26**: 647 (1982).
33. B. B. Mandelbrot, *Ann. Israel Phys. Soc.* **5**:59 (1983).
34. C. Unger and W. Klein, *Phys. Rev. B* **29**:2698 (1984).
35. D. W. Heermann and W. Klein, *Phys. Rev. B* **27**:1732 (1983).
36. D. W. Heermann and W. Klein, *Phys. Rev. Lett.* **50**:1062 (1983).